Journal of Glaciology, Vol. 26, No. 94, 1980

SNOW TRANSPORT OVER MOUNTAIN CRESTS

By Paul M. B. Föhn

(Eidg. Institut für Schnee- und Lawinenforschung, CH-7260 Weissfluhjoch/Davos, Switzerland)

Abstract. In order to gain more insight into the mountain snow-transport mechanisms wind and drift flux measurements have been executed on a ridge crest (mainly during snow-storms). Horizontal wind-speed profiles, measured between 0.3 and 6 m above snow surface, show a hump-shaped course especially for strong winds. Theoretical approximations substantiate that the Bernoullian pressure decrease on the crest may be the main cause for this type of wind profile. Roughness parameters (z_0, u_*) are determined with the aid of the wind profiles and compared with those reported in the literature. Corresponding drift density profiles coincide with steady-state drift theories as long as wind speeds are low ($u_1 \leqslant 7$–10 m s^{-1}), at greater wind speeds snow plumes of 1 to 1.5 m thickness develop immediately above snow surface. Areal measurements on snow mass-balance differences between windward and lee slopes are used to approximate the total transport over the ridge crest and to derive a quantitative relationship between crest winds and drift-snow deposition on lee slopes.

Résumé. *Transport de neige au-dessus des crêtes des montagnes.* En vue d'acquérir une meilleure connaissance des mécanismes de transport de la neige en montagne, on a exécuté des mesures de vent et de transport par le vent sur une crête montagneuse (principalement des jours de tempêtes de neige). Les profils de vitesse horizontale du vent mesurés entre 0,3 et 6 m au-dessus de la surface de la neige présentent une forme de bosse spécialement pour les vents forts. Des approximations théoriques viennent à l'appui du fait que la chute de pression de Bernoulli sur la crête peut être la cause principale de ce type de profil de vent. Les paramètres de rugosité (z_0, u_*) sont déterminés à l'aide de ces profils de vent et comparés à ceux que rapporte la littérature. Les profils correspondants de densité de chasse-neige coïncident avec les théories de l'état d'équilibre du chasse-neige tant que les vitesses de vent sont faibles ($u_1 \leqslant 7$–10 m s^{-1}), à des vitesses supérieures des plumeaux de neige de 1 à 1,5 m d'épaisseur se développent immédiatement au-dessus de la surface de la neige. On a utilisé des mesures de surface des différences entre les bilans de masse de la neige côté au vent et sous le vent, pour avoir une approximation du transport total au-dessus de la crête et pour en déduire une relation quantitative entre les vents sur la crête et le dépôt de neige sur le côté sous le vent.

Zusammenfassung. *Schneeverfrachtung über Gipfelkuppen.* Um vermehrte Einsicht in die Schneeverfrachtungsvorgänge an Gipfelkuppen zu gewinnen, wurden an einer Gratkante Wind- und Schnee-dichte-Profile gemessen. Der grösste Teil der Messungen wurde während Sturmperioden (Schneefall mit Schneetreiben) ausgeführt. Die Windprofile wiesen bei grösseren Windgeschwindigkeiten durchwegs einen bodennahen "Buckel" auf, der mit Hilfe von theoretischen Ansätzen auf den Strömungsunterdruck auf der Gratkante zurückgeführt werden konnte. Die Strömungsparameter (z_0, u_*) wurden mit Hilfe der Profile berechnet und kommentiert. Die Schneedichte-Profile stimmen mit dem bekannten Ansatz für stationäre Diffusion solange überein als geringe Windgeschwindigkeiten ($u_1 \leqslant 7$–10 m s^{-1}) vorherrschen; mit zunehmenden Windgeschwindigkeiten werden an der Gratkuppe eine Art "Schnee-Strahlströme" von 1–1,5 m Höhe beobachtet, deren Entstehung diskutiert wird. Flächenhafte Massenbilanz-Messungen der Schneedecke an ausgedehnten Luv- und Leehängen werden einerseits zur indirekten Bestimmung des gesamten Schneetransportes über die Kuppe herangezogen, andererseits dienen sie dazu eine quantitative Beziehung zwischen dem Gratwind und den mächtigen Schneeanhäufungen im Lee-Hang zu gewinnen.

Introduction

In mountainous terrain, blowing snow (taken as the combination of high-level snow-fall drift processes and low-level scoring processes) causes many problems through irregular, often excessive snow deposits. Because previous snow-drift investigations have been almost exclusively concerned with snow-drift on extended horizontal surfaces (Dyunin, 1959; Mellor, 1965; Budd and others, 1965; Radok, 1977), a study of the rather complex subject of mountain snow-drift problems has been initiated.

Our plan was to simulate the two-phase mass flux over an extended, modelled mountain crest, and, in order to achieve this, we had to design or to adapt suitable instrumentation to measure the airflow, the roughness parameters, and the snow-particle flux over a mountain crest in order to gain appropriate boundary conditions. Particle size and mass distribution also had to be measured in a separate study (Pope, 1979) as it seemed that the combination of high- and low-level snow-drifting (large snow-fall particles) would influence the catch efficiency of snow-drift gauges and hence the measured flux rates. Finally, we tried to answer

https://doi.org/10.3189/S0022143000010984 Published online by Cambridge University Press

an urgent question raised by avalanche forecasters over the years: "How much additional wind-blown snow is deposited during a snow-storm on steep lee-slopes, given the wind data on ridge-top locations?"

The main emphasis during the first phase of work was given to crest-line locations, where the eroded drift-snow of the windward slopes is passed to the leeside slopes. Thus, estimated and measured ridge-top flux rates may be compared with measured mass-balance differences on adjacent slopes yielding the possibility of cross-checking the two measuring procedures.

Test sites and instruments

All detailed wind profile, drift flux, or drift density measurements have been completed on a small crest line north of the Eidg. Institut für Schnee- und Lawinenforschung (2 670 m a.s.l.). During major snow-storm or snow-drifting periods the wind blows from the north-west across this crest line. However, because the leeside slope is disturbed by the Institut building, the areal snow re-distribution features could not be investigated on the slopes of the same ridge, but were measured on a ridge similar in orientation, shape, and slope roughly two kilometres away, the so-called Gaudergrat ridge. A cross-section of this ridge is represented in Figure 1. These two ridges show rather sharp crest lines, slope angles between 28–38°, and might be regarded as quite typical for our Alpine topography.

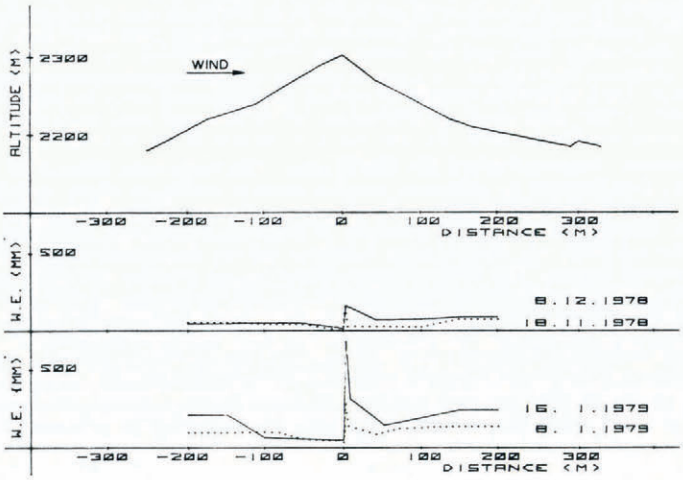

Fig. 1. Cross-section of Gaudergrat ridge (W.N.W.–E.S.E.) and mean areal mass balance for two surveyed periods. Surplus snow deposition on lee slope and irregular snow accumulation pattern may clearly be observed.

The wind profiles were measured with small cup-anemometers (accuracy ± 0.3 m s^{-1}) mounted on one side of a vertical mast, the drift-snow gauges were installed on the other side of the mast. Drift flux measurements were generally made at three heights above the snow surface (between 0.1–2 m) with a slightly modified rocket-type drift gauge first constructed and tested by Mellor (1960). The exterior shape has only been changed slightly to retain the calibrated flow efficiency ratio of 0.78 (the ratio of wind-speed through the inlet nozzle to speed in front of the nozzle). The central section of the gauge has been elongated by 10% in order to settle nearly all particles in this central region which was constructed of clear "Plexiglass" cylinders so that exposure times (0.5–2 h) could be determined visually. The sharpened inlet tube had an internal diameter of 8 mm and the separable fin section was constructed from thin aluminium sheet. (The gauges could freely turn in the vertical and

https://doi.org/10.3189/S0022143000010984 Published online by Cambridge University Press

horizontal plane to match the air flow.) The nose-to-centre velocity ratio is 306 : 1. Because the calibration measurements reported by Mellor showed that wall smoothness and wind-speed fluctuations appreciably influence the "collection" efficiency of such gauges, no corrections have been applied to the drift measurements. On a few occasions a small glass gauge of reduced size and without fins was used to gauge heights smaller than 0.1 m above snow surface.

Airflow over ridge crests

The snow-drift over crests is mainly determined by small-scale airflow, which is rarely described in the literature. Most of the theoretical work is concerned with the effects of stratification, with lee-wave phenomena, and with upper-level winds. We need measurements and a simple analytical theory which describes the interrelations between terrain shape and the turbulent boundary layer, which carries most of the suspended snow during drift conditions.

Measured wind profiles

Figure 2 shows several profiles of the horizontal wind-speed component which do not follow the usual logarithmic form. The right-hand profiles were measured almost exclusively during blowing snow periods, whereas the left-hand ones were recorded during rather sunny weather (warm-air advection). They all show a hump in the lowest metres, increasing with higher wind-speeds. Although the incomplete matching of the anemometers may account for some profile deviations, it is believed that the general trend is correct, because similar profiles, recorded with the same instruments on the adjacent windward slope during blowing snow conditions (when the wind was blowing tangentially along the slope), show a nicely logarithmic shape as one might expect for a shear flow along an inclined plane during neutral stability conditions.

In order to calculate the friction velocity u_* and the roughness length z_0 over the eroded snow surfaces, all profiles which are almost logarithmic have been analysed. Assuming the logarithmic law

$$u = (u_*/k) \ln (z/z_0), \qquad z \geqslant z_0, \tag{1}$$

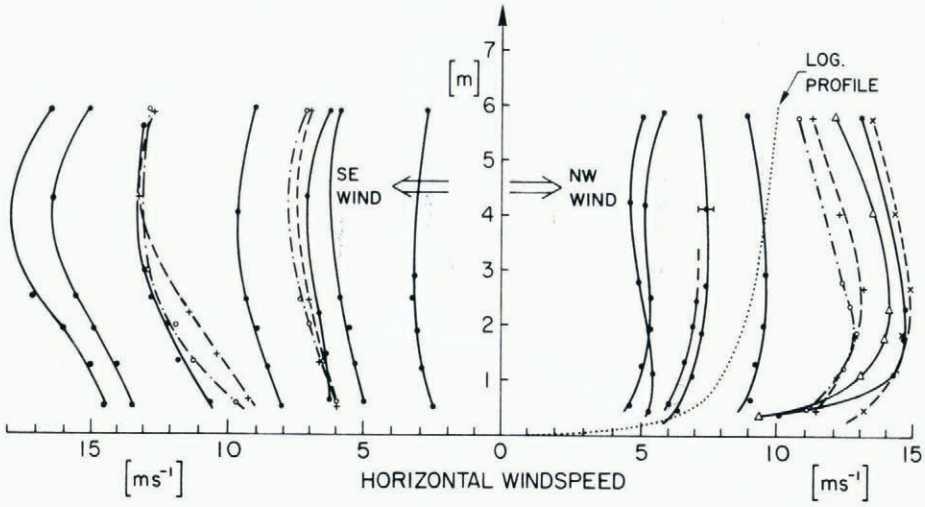

Fig. 2. A variety of vertical profiles of horizontal wind-speed measured at the Weissfluhjoch ridge crest. The wind-speed maximum is more pronounced and at a lower height if the wind approaches the ridge from N.W. than from S.E., due to terrain differences.

https://doi.org/10.3189/S0022143000010984 Published online by Cambridge University Press

where u is the wind-speed at height z and k is the von Kármán constant, the mean values for u_* and z_0 have been determined. The mean roughness length was

$$\bar{z}_0 = 1.3 \pm 1.4 \text{ mm} \qquad (\text{range } 0.04\text{–}4 \text{ mm}),$$

whereas for the friction velocity a mean value of

$$\bar{u}_* = 0.1 \pm 0.04 \text{ m s}^{-1} \qquad (\text{range } 0.04\text{–}0.18 \text{ m s}^{-1}),$$

was evaluated. The wind-speed range was 5–15 m s^{-1} at a height of one metre. The number of "logarithmic" wind profiles was rather limited due to the special measuring locations ($N = 12$), and so no attempt was made to derive a general relationship of the form $z_0 = f(u_*)$; similarly a simple linear expression:

$$u_* = 0.02 u_z,$$

was chosen for the relationship between u_* and a reference velocity u_z, a form often quoted in the literature (Mellor, 1965; Shiotani and Arai, 1967).

The mean value of z_0 corresponds to the larger values reported previously (Deacon, 1953; Budd and others, 1965; Ōura and others, 1967), the value of $\bar{u}_*$ is, according to Mellor (1965), two to four times smaller than those usually reported. These divergences could indicate that even the selected profiles had a small hump-like deviation at lower heights, thus increasing z_0 and reducing u_*. The Sutton criterion for aerodynamically rough flow

$$\frac{u_* z_0}{\nu} > 2.5, \tag{2}$$

where ν is the kinematic viscosity of air, was always fulfilled.

Theoretical approach

Strong airflow ($u_1 > 7$ m s^{-1}) seems to cause an accelerated, hump-shaped wind profile on ridge-top locations. It is well known that neither potential flow nor viscous flow theories describe the boundary layer flow adequately, but such theories may describe the contribution of the various forces which are important for the flow of snow particles in the air stream.

According to Prandtl (1965, p. 523) a boundary-layer equation may be derived from the hydrodynamic equations of motion and continuity. A sketch of the flow field and the coordinate-system appears in Figure 3. Beginning from an incompressible fluid moving in the x-direction with a mean velocity u or U_0, the equation may be written for steady two-

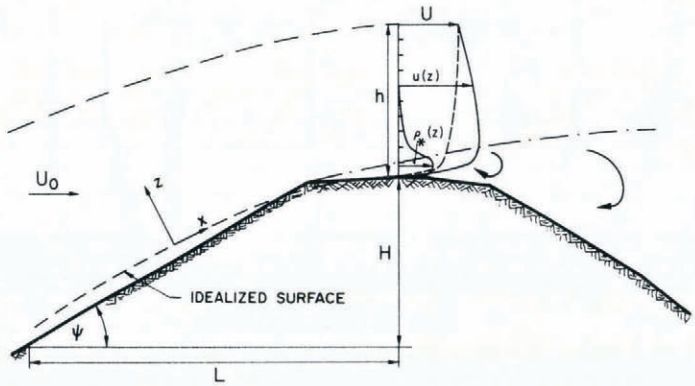

Fig. 3. Schematic diagram of turbulent-flow regime and snow-drift concentration on a ridge crest.

https://doi.org/10.3189/S0022143000010984 Published online by Cambridge University Press

dimensional flow (assuming a predominance of the x-direction terms over those in the z-direction):

$$\rho'\left(u\frac{\partial u}{\partial x}+v\frac{\partial u}{\partial z}\right)=\rho' g-\frac{\partial p}{\partial x}+\frac{\partial \tau_{zx}}{\partial z}, \tag{3}$$

where u and v are the x- and the z-velocity components, g is the acceleration due to gravity, ρ' is the air density including drifting snow, and p and τ_{xz} the pressure and Reynolds stress, respectively. If no abrupt slope changes occur, the local curvatures of the boundary layer of depth h may be neglected, i.e. the x-coordinate is positioned along the slope.

The first term on the right-hand side represents the effect of the weight, the second a volume force (the Bernoulli pressure-gradient force), and the third the frictional forces; the left-hand-side terms represent the inertial forces.

We can see that mainly inertial forces (almost frictionless flow) are experienced in the uppermost air layer above the ridge, whereas in the lower layer (between the two dashed lines in Fig. 3) predominantly frictional forces are present despite the fact that air is a medium of low viscosity. Because the major snow-transport phenomena take place in this lower layer, special attention is given to this layer in what follows. For the upper boundary, applying Bernoulli's equation:

$$p+\rho'\frac{U^2}{2}=\text{constant},$$

and we may write:

$$\frac{\partial p}{\partial x}=-\rho' U\frac{\partial U}{\partial x}, \tag{4}$$

where U is the speed of the upper, almost frictionless flow.

At the lower boundary (where $u=v=0$) the equation may be written as:

$$\frac{\partial p}{\partial x}=\frac{\partial \tau_{zx}}{\partial z}. \tag{5}$$

Generally speaking, the boundary conditions are:

at $z=0$, $u=0$

at $z=h$, $u=U$, and $\dfrac{\partial u}{\partial z}=0$.

Knowing that the atmospheric boundary-layer equations may only be solved analytically provided the specific problem can be formulated in terms of ordinary differential equations, we try to find a solution for the ridge-top wind profile with appropriate simplifications.

If we consider only the much larger turbulent part of the frictional stresses, the term τ_{zx}, following Prandtl's theory of momentum transfer, may be written as

$$\tau_{zx}'=\rho' l^2\left|\frac{\partial u}{\partial z}\right|\frac{\partial u}{\partial z}.$$

We set

$$\mu'=\rho' l^2\left|\frac{\partial u}{\partial z}\right|, \tag{6}$$

and for the new coefficient of eddy viscosity μ' the expression

$$\mu'=\rho' k(z+z_0)\,u_* \tag{7}$$

can be derived where l is a distance known as the mixing length.

https://doi.org/10.3189/S0022143000010984 Published online by Cambridge University Press

Equation (3) may be rearranged to formulate an equation for the ridge-top location, where all horizontal gradients of the mean velocity are much smaller than the vertical ones; gravity forces are negligible due to the small density differences:

$$\mu' \frac{\partial^2 u}{\partial z^2} - \rho' v \frac{\partial u}{\partial z} = \frac{\partial p}{\partial x}. \tag{8}$$

This equation may be solved for $u(z)$ by introducing for μ' the values given in Equation (7), by assuming that v is a small and constant term on ridge-top locations and by applying for $\partial p/\partial x$ a numerical value derived from the specific ridge dimensions.

A solution which satisfies the boundary conditions is of the form:

$$\left.\begin{aligned} u &= \frac{u_*}{k} \ln \frac{z}{z_0} - \frac{h}{\rho' k z_0 u_*} \frac{\Delta P}{\Delta x} \left\{ z_0 - z \left(\frac{z_0}{h} \right) \right\}, \\ z_0 &\leqslant z \leqslant h, \end{aligned}\right\} \tag{9}$$

where h is the boundary-layer height and $\Delta P/\Delta x$ is the local "Bernoulli" pressure gradient.

The local pressure gradient may be approximated by Equation (4) using for U an empirical relation for a wedge-shaped surface given by Mangler (1948) in the form

$$U = U_0 \left(\frac{3x}{L \sin^2 \psi} \right)^{0.17}, \tag{10}$$

and further

$$\frac{dU}{dx} = \frac{0.17U}{x}, \tag{11}$$

where U_0 stands for the free-air flow speed, L is the windward base distance of the ridge, and ψ the mean slope angle.

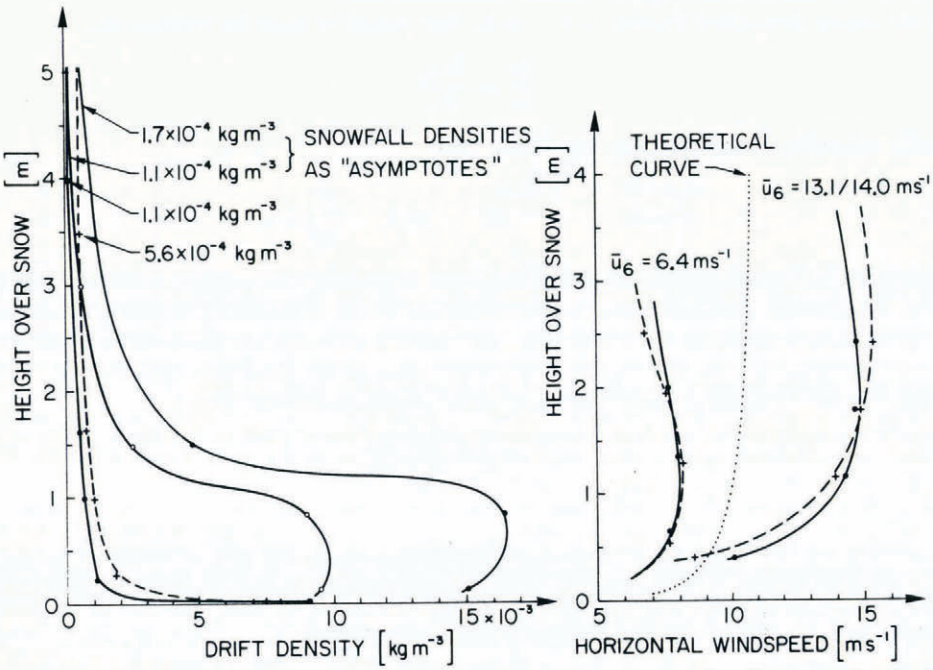

Fig. 4. Typical drift density profiles are shown on the left together with corresponding wind profiles measured on the ridge crest on the right. The theoretical wind-profile curve, calculated using Equation (9) bulges less than the measured ones and yields a flat maximum at a height of about 4 m.

https://doi.org/10.3189/S0022143000010984 Published online by Cambridge University Press

In order to simulate the mean measured wind conditions of Figure 4 a free-flow speed $U_0 = 10$ m s^{-1}, a ridge length of $x = 180$ m and a boundary-layer height of 8 m were used. The theoretical curve of Figure 4 shows, in comparison with the measured wind profiles, that part of the humped-shaped profiles may be explained by theory, but that the measured profiles bulge even more, perhaps an indication that additional small-scale geometrical effects may be involved (e.g. small surface edges caused by cornices).

Measurements of blowing snow

A theoretical analysis of the transport of blowing snow over a mountain ridge, combining the equations of motion, continuity, and the diffusion equations, could not be accomplished, so in the following section only the measured drift-flux profiles converted to drift-density profiles will be discussed. Figure 4 shows on the left-hand side four selected drift-density profiles, recorded on the same ridge-top location during snow-storms with low to moderate snow-fall densities. The corresponding wind profiles are given in the right-hand side of Figure 4.

The "low wind-speed" density profiles (two additional ones are presented in detail on Figure 5) conform approximately to the theoretical steady-state snow-drift relation first published by Shiotani and Arai (1967)

$$\rho_* = \rho_{*1}\left(\frac{z}{z_1}\right)^{-w/ku_*}, \tag{12}$$

where ρ_*, ρ_{*1} are snow-drift densities at the levels z, z_1 respectively, and w is the terminal velocity of the particles, chosen according to literature (Hobbs and others, 1973) as 0.5 m s^{-1}.

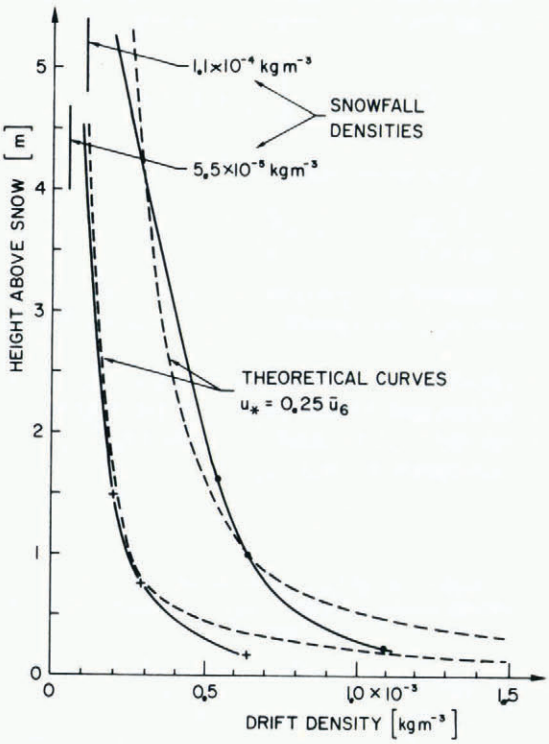

Fig. 5. Two measured drift-density profiles, which show similar shape to the theoretical steady-state drift profiles, if friction velocity u_* (obtained by wind measurements) is enlarged by an order of magnitude.

https://doi.org/10.3189/S0022143000010984 Published online by Cambridge University Press

However, the two detailed profiles of Figure 5 could not have been matched with theoretical curves if the mean measured friction velocities relationship for the wind profiles

$$u_* = 0.02u_6,$$

had been used, where u_6 represents the wind-speed at a height of 6 m above snow surface. A u_* enhanced approximately by a factor of ten

$$u_*' = 0.25u_6,$$

was required to match the curves roughly. It is interesting to note that Sommerfeld and Businger (1965) have shown that the ratio of the eddy diffusivity for blowing snow K_s and the eddy viscosity K_m derived from wind profiles is also 10 : 1.

As indicated in the previous sections, one objective of the present study was to estimate the areally measured transport rates over the ridge crest (mass balance between windward and leeward slopes) by measured drift transport rates on the crest line.

The calculation of the drift transport

$$Q = \int_{z_0}^{z_u} \rho_*(z)\, u(z)\, \mathrm{d}z,$$

or the specific drift transport

$$\bar{Q} = \frac{1}{z_u - z_0} Q,$$

which yields the mean transport rate per unit area, readily comparable with areal measurements, is straightforward once the height limits are chosen:

$$\bar{Q} = \frac{1}{z_u - z_0} \int_{z_u}^{z_0} \rho_*(z)\, u(z)\, \mathrm{d}z, \tag{13}$$

where z_u is the upper and z_0 the lower height limit.

$$\bar{Q} = \frac{1}{z_u - z_0} \left\{ \frac{\rho_{*1} u_*}{k(1-a)} \left(z_u^{1-a} \left(\ln \frac{z_u}{z_0} - \frac{z_0}{1-a} \right) + \frac{z_0}{1-a} z_0^{1-a} \right) \right\}, \tag{14}$$

where $a = w/ku_*'$, a term defined in Equation (12), now slightly modified for blowing snow with u_*' in the denominator, ρ_{*1} corresponds to the measured drift density at the one-metre level.

The specific drift transport rates and the drift density ρ_{*0} at the height $z_0 = 10^{-3}$ m have been calculated for the two drift profiles represented in Figure 5 and are given in Table I. For the main calculations the "pure" drift densities (ρ_{*1}', ρ_{*0}'), i.e. snow-fall densities subtracted first, have been considered (e.g. $\rho_{*1}' = \rho_{*1} - \rho_p$, where ρ_p is the precipitation density).

TABLE I. CALCULATED z_0 DRIFT DENSITIES (ρ_{*0}'), SPECIFIC DRIFT TRANSPORT RATES FOR VARIOUS LAYER HEIGHTS ($\bar{Q}_{z^{z_{u_0}}}$) AND COMBINED SNOW-FALL–SNOW-DRIFT TRANSPORT RATES FOR WINDSPEEDS OF 6 AND 12 m s^{-1}

u_6 m s^{-1}	ρ_{*1}' $\times 10^{-3}$ kg m^{-3}	ρ_{*0}' $\times 10^{-3}$ kg m^{-3}	$\bar{Q}_{z_0^1}$	$\bar{Q}_{z_0^5}$ $\times 10^{-3}$ kg m^{-2} s^{-1}	$\bar{Q}_{z_0^{40}}$	$\bar{Q}_{z_0^{300}}$	$\bar{Q}_p$ $\times 10^{-3}$ kg m^{-2} s^{-1}	$\bar{Q}_{z_0^{40}}+\bar{Q}_p$
6	0.20	63	5.7	1.8	0.4	0.09	0.33	0.73
12	0.20	3.6	3.3	2.1	1.1	0.55	0.66	1.76
6	0.54	171	15.4	5.0	1.1	0.24	0.66	1.76
12	0.54	9.6	8.8	5.6	2.8	1.50	1.32	4.12

https://doi.org/10.3189/S0022143000010984 Published online by Cambridge University Press

A comparison with measured values by Budd and others (1966) shows that for rather low wind-speeds on the ridge (6–12 m s^{-1}) the extrapolated z_0 drift densities (ρ_{*0}') are an order of magnitude smaller than on flat Antarctic snow-fields. In addition Table I illustrates that the specific drift transport rate depends strongly on the upper height limit, especially for low wind speeds. If we choose an upper height limit of 40 m as adequate based on visual observations, we see that the specific drift transport rates may be doubled through slight snow-fall drift (0.1–0.2 mm water equivalent h^{-1}). Snow-fall densities have been calculated with the aid of three snow-fall precipitation recording gauges, positioned on a flat sheltered experimental plot in the vicinity of the ridge.

More typical drift density profiles on crest-line locations are shown in Figures 3, 4, and 6. As soon as the crest wind-speed reaches a threshold velocity of $u_1 = 7$–10 m s^{-1}, the drift density profiles also show a hump-shaped course. The left side of Figure 6 demonstrates the

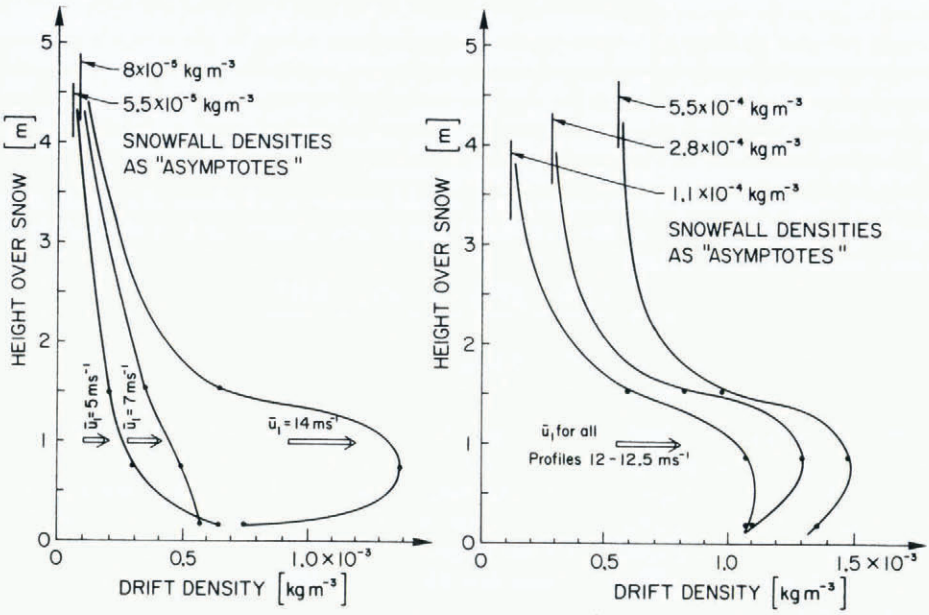

Fig. 6. Measured drift-density profiles: left-hand side shows the effect of increased winds; right-hand side illustrates translatory shift by increased snow-fall rates. (A snow-fall density of 5.5×10^{-4} kg m^{-3} corresponds to about 1 mm water equivalent snow per hour.)

transition from a steady-state snow-drift profile to a typical crest-line drift profile with increasing velocities. The right side of Figure 6 illustrates the fact that snow-fall, i.e. an additional precipitation snow flux may be superimposed on low-level scoring processes, thus the measured drift profiles are only translated by the snow-fall.

The hump-shaped density profiles may be caused by the flow acceleration over the top of the ridge (cf. wind profiles) leading to reduced pressure and therefore increased particle lift. Another explanation for a uniform snow-filled ground layer of 1–1.5 m depth above snow surface could be based on the presence of a separation layer, starting at the edge of the ridge as illustrated in Figure 3. Drift measurements on ridges of different microshapes and theoretical approximations, e.g. turbulent motion theories of buoyant jets and plumes, may clarify this point in future.

https://doi.org/10.3189/S0022143000010984 Published online by Cambridge University Press

Determination of snow transport by areal mass balances

In connection with a study into the influences of slope aspect on the stability of seasonal snow cover, re-distribution of loose surface snow and the deflection of suspended snow have been analysed on an extended ridge similar in shape and orientation to the one described in the previous sections. It is obvious that the measured snow mass-balance differences between an extended windward slope and the adjacent lee slope may help to approximate the total transport over the crest as well as to localize typical avalanche-prone snow deposits.

During the winter 1978–79 more detailed areal measurements have been initiated in anticipation of suitable snow-storm conditions (steady winds from W.N.W.–N.W., lasting for a few days and dumping enough snow for the measuring error to be small). Unfortunately such periods occurred rarely this winter, the wind regime was unsteady in direction, and speed and snow-fall rates were low compared with previous winters. However, a few periods could be analysed separating time spans with low wind-speeds and no drift phenomena from those with blowing snow conditions.

There are basically three possibilities involved in estimating the specific transport rate from the windward onto the lee slope and, as a consequence, the windborne mean snow deposition in the lee slope D. Either the snow loss in the windward slope ΔW_{W} or the snow gain on the lee slope ΔW_{L} compared with a horizontal, drift-free snow plot ΔW is determined during blowing snow periods; furthermore a mean value of both may be chosen as an even better estimate counterbalancing the measuring errors.

Assuming that a snow-storm without wind would deliver to all slopes the same amount of snow and that, by definition, on the windward slope snow erosion and on the lee slope snow deposition occur, we may write:

$$D = \frac{(\Delta W - \Delta W_{\mathrm{W}}) + (\Delta W_{\mathrm{L}} - \Delta W)}{2}, \tag{15}$$

$$D = \frac{\Delta W_{\mathrm{L}} - \Delta W_{\mathrm{W}}}{2}. \tag{16}$$

The arithmetic mean of the two terms in Equation (16) is equivalent to the net mass gain on the horizontal snow plot and may be used as a measure for the tightness of the whole system. If the measured mass increase (ΔW) on the horizontal plot shows values within $\pm 10\%$ of the above mean, we may conclude that no essential gain or loss of snow mass takes place from or towards areas outside the surveyed slope areas.

If $(\Delta W_{\mathrm{L}} + \Delta W_{\mathrm{W}})/2 < \Delta W$ mass losses are likely, if $(\Delta W_{\mathrm{L}} + \Delta W_{\mathrm{W}})/2 > \Delta W$ mass gains must be assumed.

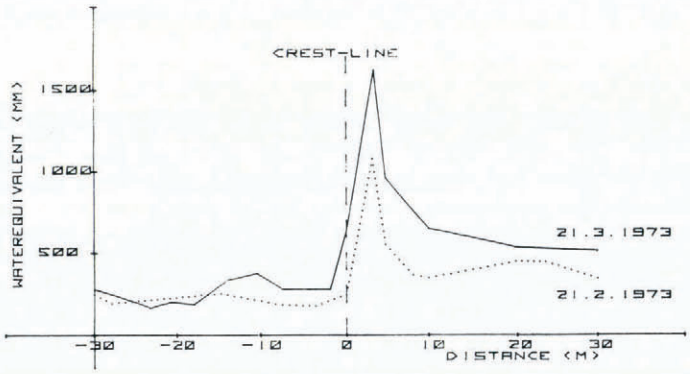

Fig. 7. Mean areal snow-cover water equivalent in the upper part of Gaudergrat ridge on two consecutive dates. Windward slope (left to crest-line) stores appreciably less snow than leeward slope (right side of crest line).

https://doi.org/10.3189/S0022143000010984 Published online by Cambridge University Press

Figure 7 shows an example of such areal mass balance measurements in the immediate vicinity of the crest-line. The whole outlined time interval consisted of three blowing-snow periods with moderate winds (mean daily wind speeds between 5 and 13 m s^{-1}) and yielded the following total mass gains:

windward slope	leeward slope	horizontal plot
61 kg m^{-2}	236 kg m^{-2}	125 kg m^{-2}.

Consequently mean lee-slope snow deposition by blowing snow amounts to $D = 87.5$ kg/m², whilst for the specific drift transport rate $\bar{Q}$ a mean value of 1.04×10^{-3} kg m^{-2} s^{-1} results. This amount compares favourably with the values of $\bar{Q}_{z_0{}^{40}}$ in Table I.

Two additional examples, where the slopes have been surveyed further up- and down-wind are represented in Figure 1. Using these two representative periods as a basis for discussion, the following features may be of interest:

A horizontal distance of about 200 m on both sides of the crest-line seems to contain in most cases the blowing-snow processes caused by the ridge.

If the mass ratio

$$\frac{(\Delta W_{\mathrm{L}} + \Delta W_{\mathrm{W}})/2}{\Delta W} \neq 1$$

(system not closed), then it is rather smaller than one, indicating that mass losses are mainly on the lee side (sublimation and/or drifting snow further down-wind).

In the wind shadow of the ridge there is a strong reverse eddy flow of the order of 50 to 150 m long (measured horizontally, Fig. 1), resulting in a large depression or cavity in the snow-pack. Where snow-pack depth is substantially decreasing, zones of increased stresses develop, often giving rise to snow-slab failure.

Surveying the mass balance on ridge slopes before and after snow-storm periods and including the ridge-crest wind data, quantitative relationships for the surplus deposition of snow in the upper parts of lee slopes may be derived. The wind power, the expression of the ability of the wind to transport snow is, theoretically, proportional to the cube of the wind-speed, thus an empirical relationship of the form

$$H_{NS} = k\bar{u}^3 \ \{\mathrm{m\ d^{-1}}\}, \qquad \bar{u} \leqslant 20 \ \mathrm{m\ s^{-1}}, \tag{17}$$

may be established. H_{NS} represents an average areal "wind-snow" depth, i.e. the surplus snow accumulation by wind on lee slopes compared with drift-free horizontal areas. The coefficient $k = 8 \times 10^{-5}$ s^3 d^{-1} m^{-2} is determined empirically. The relation holds for snow-storm conditions and for periods of 24 h, consequently for $\bar{u}$ the mean daily wind-speed on the crest has to be inserted. The introduction of a threshold velocity, above which snow transport is said to begin (cf. Dyunin, 1959) was not adequate, because during snow-storms snow particles are fed into the air flow from upper air layers even at very low wind speeds.

Equation (17) has been derived from mass-balance measurements over three winters (1972/73–1974/75) on the ridge described here and it may be of interest that the few short-interval measurements of the past winter (1978/79) confirmed the validity of this approximation.

Conclusions

The problem of snow erosion or drift accumulation by natural topographical features is great, a primary requirement for its solution is a quantitative estimate of air-flow patterns over various terrain structures. It has not been possible here to do more than mention a few problems, however the measurements and theoretical approximations presented may help to begin further work in mountainous terrain.

The most important points can be summarized as follows:

https://doi.org/10.3189/S0022143000010984 Published online by Cambridge University Press

Profiles of the horizontal wind-speed measured on a ridge show a hump-shaped course close to the ground with a wind-speed maximum between 1 and 4 m height. Mean measured surface roughness z_0 amounts to 1.3 mm and seems to be independent of snow surface features. Mean friction velocity $\bar{u}_*$ equals 0.1 m s^{-1} or in terms of the wind speed at 6 m, $\bar{u}_* = 0.22u_6$, on the other hand the blowing-snow friction velocity u_*' seems to be an order of magnitude larger, consequently the relationship $u_*' = 0.25u_6$ may be used.

A theoretical solution of Prandtl's boundary-layer equation adapted for the specific ridge-crest conditions shows that the negative pressure gradient towards the ridge crest might be the main cause for the special wind profile.

An elongated rocket-shaped drift gauge (Mellor, 1960) is well suited for drift-flux measurements on ridge crests. Riming occurred rarely and the large snow particles of Alpine snow storms could easily enter the inlet nozzle.

Drift-density profiles measured at the ridge crest conform roughly with theoretical steady-state drift profiles providing wind speeds are low ($u_1 \leqslant 7$–10 m s^{-1}), at greater wind-speeds a snow plume of 1–1.5 m depth develops above the snow surface. It may be explained partly by accelerated air flow and/or by small-scale geometric effects (flow separation by small surface edges).

Areal mass balance measurements of storm periods yield the possibility of cross-checking measured or theoretically approximated ridge-crest flux rates. At the same time they may be used to derive much needed quantitative relationships between crest winds and drift-snow deposition on lee slopes.

ACKNOWLEDGEMENTS

I am very grateful to R. Meister and M. Pope for their assistance in the field and for executing various computer studies.

REFERENCES

Budd, W. F., *and others*. 1965. The Byrd snow drift project: outline and basic results, by W. F. Budd, [W.] R. [J.] Dingle, and U. Radok. (*In* Rubin, M. J., *ed*. *Studies in Antarctic meteorology*. Washington, D.C., American Geophysical Union, p. 71–134. (Antarctic Research Series, Vol. 9.))

Deacon, E. L. 1953. Vertical profiles of mean wind in the surface layers of the atmosphere. *Geophysical Memoirs* (London), Vol. 11, No. 91.

Dyunin, A. K. 1959. Osnovy teorii meteley [Fundamentals of the theory of snow drifting]. *Izvestiya Sibirskogo Otdeleniya Akademii Nauk SSSR*, Tom 12, 1959, p. 11–24. [English translation: *Canada. National Research Council. Technical Translation* 952, translated by G. Belkov, 1961.]

Hobbs, P. V., *and others*. 1973. A theoretical study of the flow of air and fallout of solid precipitation over mountainous terrain: pt. 2. Microphysics, [by] P. V. Hobbs, R. C. Easter, and A. B. Fraser. *Journal of the Atmospheric Sciences*, Vol. 30, No. 5, p. 813–23.

Mangler, W. 1948. Zusammenhang zwischen ebenen und rotationssymmetrischen Grenzschichten in kompressiblen Flüssigkeiten. *Zeitschrift für angewandte Mathematik und Mechanik*, Bd. 28, Ht. 4, p. 97–103.

Mellor, M. 1960. Gauging Antarctic drift snow. (*In Antarctic meteorology. Proceedings of the symposium held in Melbourne, February 1959*. London, Pergamon Press, p. 347–55.)

Mellor, M. 1965. Blowing snow. U.S. Cold Regions Research and Engineering Laboratory. *Cold regions science and engineering*. Hanover, N.H., Pt. III, Sect. A3c.

Ōura, H., *and others*. 1967. Studies on blowing snow. II, by H. Ōura, T. Ishida, D. Kobayashi, S. Kobayashi, and T. Yamada. (*In* Ōura, H., *ed*. *Physics of snow and ice: international conference on low temperature science. . . . 1966. . . . Proceedings*, Vol. 1, Pt. 2. [Sapporo], Institute of Low Temperature Science, Hokkaido University, p. 1099–117.)

Pope, M. 1979. Particle size and mass distribution in Alpine windblown snow. *Interner Bericht des Eidg. Institutes für Schnee- und Lawinenforschung*, Nr. 567.

Prandtl, L. 1965. *Führer durch die Strömungslehre. Sechste Auflage*. Braunschweig, Verlag F. Vieweg und Sohn.

Radok, U. 1977. Snow drift. *Journal of Glaciology*, Vol. 19, No. 81, p. 123–39.

Shiotani, M., *and* Arai, H. 1967. On the vertical distribution of blowing snow. (*In* Ōura, H., *ed*. *Physics of snow and ice: international conference on low temperature science. . . . 1966. . . . Proceedings*, Vol. 1, Pt. 2. [Sapporo], Institute of Low Temperature Science, Hokkaido University, p. 1075–83.)

Sommerfeld, R. A., *and* Businger, J. A. 1965. The density profile of blow snow. *Journal of Geophysical Research*, Vol. 70, No. 14, p. 3303–06.

https://doi.org/10.3189/S0022143000010984 Published online by Cambridge University Press